



HAL
open science

Mechanical properties of heat-treated organic foams

G. Amaral-Labat, Muhammad Sahimi, Antonio Pizzi, Vanessa Fierro, Alain Celzard

► **To cite this version:**

G. Amaral-Labat, Muhammad Sahimi, Antonio Pizzi, Vanessa Fierro, Alain Celzard. Mechanical properties of heat-treated organic foams. *Physical Review E: Statistical, Nonlinear, and Soft Matter Physics*, 2013, 87 (3), 10.1103/PhysRevE.87.032156 . hal-01296308

HAL Id: hal-01296308

<https://hal.science/hal-01296308>

Submitted on 21 Apr 2020

HAL is a multi-disciplinary open access archive for the deposit and dissemination of scientific research documents, whether they are published or not. The documents may come from teaching and research institutions in France or abroad, or from public or private research centers.

L'archive ouverte pluridisciplinaire **HAL**, est destinée au dépôt et à la diffusion de documents scientifiques de niveau recherche, publiés ou non, émanant des établissements d'enseignement et de recherche français ou étrangers, des laboratoires publics ou privés.



Distributed under a Creative Commons Attribution 4.0 International License

Mechanical properties of heat-treated organic foams

G. Amaral-Labat,¹ Muhammad Sahimi,^{2,*} A. Pizzi,³ V. Fierro,¹ and Alain Celzard^{1,†}

¹*Institut Jean Lamour - UMR CNRS 7198, CNRS - Nancy-Université - UPV-Metz, Département Chimie et Physique des Solides et des Surfaces, ENSTIB, 27 rue Philippe Séguin, Boîte Postale 1041, 88051 Épinal cedex 9, France*

²*Mork Family Department of Chemical Engineering and Materials Science, University of Southern California, Los Angeles, California 90089-1211, USA*

³*LERMAB - ENSTIB, 27 rue Philippe Séguin, Boîte Postale 91067, 88051 Epinal cedex 9, France*

(Received 12 November 2012; revised manuscript received 22 February 2013; published 25 March 2013)

The mechanical properties of a class of cellular material were measured. The composition of the material was progressively modified, while its pore structure was kept unchanged. Rigid foam, prepared from a thermoset resin, was gradually converted into reticulated vitreous carbon foam by pyrolysis at increasingly higher heat-treatment temperatures (HHT). The corresponding changes in the Young's modulus Y and the compressive strength σ of the materials were measured over a wide range of porosities. The materials exhibit a percolation behavior with a zero percolation threshold. At very low densities the Young's modulus and the compressive strength appear to follow the power laws predicted by percolation theory near the percolation threshold. But, whereas the exponent τ associated with the power-law behavior of Y appears to vary significantly with the material's density and the HHT, the exponent associated with σ does not change much. The possible cause of the apparent and *surprising* nonuniversality of τ is discussed in detail, in the light of the fact that only the materials' composition varies, not the structure of their pore space that could have caused the nonuniversality.

DOI: [10.1103/PhysRevE.87.032156](https://doi.org/10.1103/PhysRevE.87.032156)

PACS number(s): 64.60.ah, 81.05.Rm, 62.20.de

I. INTRODUCTION

There are currently several models that may be used for explaining and predicting the physical properties of two-phase disordered materials. In particular, the percolation model [1,2] has been invoked extensively in order to study various phenomena in such materials. But, to quote Ref. [2], although “percolation theory has been applied to a number of phenomena, it has not always been possible to compare its predictions with experimental data, and consequently it has not always been possible to check the quantitative accuracy of the predictions.” The predictions of other models and theories agree sometimes with those provided by percolation theory, but they either lead to different interpretations than what is provided by percolation, or still need to be confirmed by experimental data. Hence, numerical simulation has remained a crucial tool for accepting or rejecting such models, as well as testing the limits of the theoretical predictions. But, experimental measurements, carried out with materials that are used in various applications, remain the most accurate way of testing a given theory or model, provided that their structure and composition are controlled precisely. This has motivated experimentalists to test the predictions of various theories [3,4] for the properties of heterogeneous materials.

As an important example, the elastic properties of three-dimensional (3D) disordered materials in the vicinity of their rigidity [5,6] or percolation threshold [4,7,8] have been described in terms of power laws and the critical exponents of percolation [1,2]. It has been proposed that the numerical value of the exponent τ that characterizes the power-law behavior of

the elastic moduli Y near the rigidity or percolation threshold,

$$Y \sim (p - p_c)^\tau, \quad (1)$$

where p is the (volume) fraction of the rigid phase and p_c is the rigidity or percolation threshold, may be related to the nature of the microscopic elastic forces that are involved. In two-dimensional systems [4], [7,8], $\tau \simeq 3.96$ for both rigidity percolation that involves only central (stretching) forces (CF) and those that are governed by the CF and angle-changing or bond-bending (BB) forces, whereas $\tau \simeq 3.8$ for 3D systems with both the CF and BB forces [8], which has been consistent with the experimental data [9], but the most accurate estimate of τ that is currently available [6] is $\tau \simeq 2$ if only the CF are predominant. Other values of τ have also been reported [4] for, for example, some chemical gels [10], but have been interpreted differently, including, for example, the possibility that some of such materials have fractal pores [11].

As for the compressive strength σ of such materials, an exponent ζ is defined by

$$\sigma \sim (\phi - \phi_c)^\zeta, \quad (2)$$

where ϕ and ϕ_c are, respectively, the density and its critical value at the threshold. The numerical value of ζ is mostly between two theoretical limits: 1.5 for open cells and 2 for closed ones. But, an exponent of 1.36 has also been reported for describing rigid foams, based on a packing of hollow spheres [12]. Thus, despite nearly three decades of theoretical and experimental work, as well as high-precision computer simulations, the question of the universality class of the elastic properties of two-phase materials with a rigidity or percolation threshold has not been solved completely. Interpreting the experimental data that do not seem to fall in the proposed universality classes is another unsolved question. In order to be able to do so, it is necessary to have a material for which the nature of the microscopic elastic forces can be

*moe@usc.edu

†Also at the Institut Universitaire de France; Alain.Celzard@enstib.uhp-nancy.fr



FIG. 1. (Color online) Foaming sequence of tannin-based resin. Elapsed time is 1 min.

gradually changed without any modification to its structure. If percolation theory is truly applicable, then the critical exponent of the elastic moduli should belong to one of the theoretically well-understood universality classes. In contrast, if the models based on the pore topology are valid, then the exponent that characterizes the fracture strength of the material should remain constant, as the nature of the microscopic forces changes.

But, the currently-used cellular materials present serious limitations for use as models in the framework of such studies. Available rigid foams, such as polymers, ceramics, or metals, cannot have different compositions for a given fixed porous structure, hence the impossibility of changing the nature of the microscopic elastic forces. In the present paper, the mechanical properties of highly porous rigid foams, derived from tannins, are reported and interpreted. The materials were prepared from a thermoset resin that can be pyrolyzed at various temperatures, leading to foams of different compositions whose cellular structure remains constant [13]. Thus, we have studied the corresponding changes in the elastic moduli and the compressive strength of these materials.

The rest of the paper is organized as follows. Section II is dedicated to the description of the porous materials, their precursors, and synthesis. The techniques for investigating the rigid foams are also described, and what is already known for such cellular solids is recalled. The results are described and discussed in Sec. III, after which the paper is summarized.

II. MATERIALS AND METHODS

We first describe the synthesis of the materials that we study, after which their main characteristics are discussed. The experimental procedure for measuring the mechanical properties is then explained.

A. Synthesis of the rigid foams

The rigid foams were prepared from commercial flavonoid tannins, a low-cost natural resource, industrially extracted from wattle barks. Flavonoids present the same kind of reactivity as resorcinol and phenol, two synthetic and toxic molecules with which resins are traditionally prepared. In the experiments tannin (the base for resin) was mixed with water (the solvent), furfuryl alcohol (heat generator during its polymerization with itself and with tannin), formaldehyde (the cross-linker), and diethyl ether (the blowing agent). After homogenizing the mixture, sulphonic acid (the catalyst) was added, leading to the polymerization of furfuryl alcohol and tannin. The heat generated by the reaction induced boiling of ether and, hence, the bulging of the foam in one direction. Because of formaldehyde, hardening occurred as soon as foaming was completed, so that the foam neither cracked nor

collapsed. The foaming sequence is shown in Fig. 1. More details about the preparation protocol and the amounts of chemicals needed were given in the recent works [13–16].

Foams with several bulk densities, ranging from 0.04 to 0.13 g/cm³, were prepared using the required amounts of the blowing agent. Two important correlations have recently been established [13] for such materials: (i) their bulk density is inversely proportional to the amount of the blowing agent, and (ii) their average cell size is inversely proportional to the bulk density. In other words, both density and cell size are predictable, on average, given the amount of the blowing agent. Slightly different densities can, however, be obtained, depending on the zone of the foams in which the samples are cut off.

The foams were then aged for completion of the polymerization reactions. Then, parallelepiped samples were cut off and submitted to pyrolysis. The experiments were carried out at six heat-treatment temperatures (HTT), namely, 200, 400, 600, 800, 1000, 1200, and 1400 °C, but the data obtained in a previous work [17] at HTT = 900 °C are also reported here, in order to make the set of data used in the analysis more complete. The pyrolysis of each sample was carried out in an electric tubular furnace, continuously flushed with high-purity argon. The samples were always heated at 4 °C/min until the required HTT was reached, and the latter was maintained for 2 h before the furnace was switched off for cooling under argon flow. Note that the properties of non-heat-treated samples (those prepared at room temperature) were also investigated.

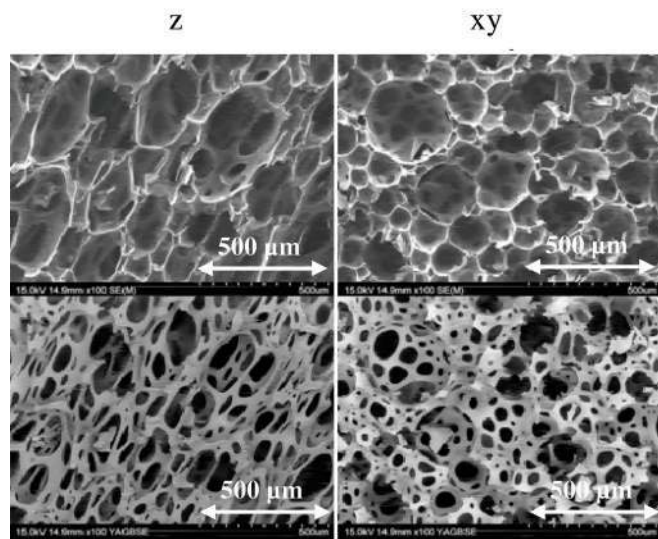
B. The foams' characteristics

Due to the vertical bulging of the foam, the samples were always slightly anisotropic, so that two main directions were defined before the pyrolysis. The growth axis was denoted by z , while the planes orthogonal to the growth direction were the xy planes [see Fig. 2(a)]. Observations through a scanning electron microscope (SEM) confirmed that the cells are slightly elongated along the z direction [see Fig. 2(b)]. Moreover, such anisotropy has been reported for all the physical properties measured so far [18] (see also below).

In recent works [17,18] we showed that during the pyrolysis the porous structure of the materials that we prepare remains unchanged. Pyrolysis only gradually transforms the organic resin into glasslike carbon without any change in its morphology. Only isotropic shrinkage was observed during the process. After the synthesis, the composition of the organic foam was roughly CH_{0.91}O_{0.43}S_ε, with $\epsilon < 5 \times 10^{-3}$. When the HTT increases, the H, O, and S atoms are progressively volatilized, leading to a hard vitreous material whose elemental carbon content is around 95%. Most of the weight loss during the pyrolysis occurred below 500 °C (see Fig. 3). The



(a)



(b)

FIG. 2. (Color online) Anisotropy of the foams. (a) Definition of the two principal directions after foaming. (b) The structural anisotropy as seen by SEM, using secondary electrons best imaging cells and pore walls (top), or backscattered electrons best imaging struts and connections between cells (bottom).

insulator-conductor transition occurs around 750 °C only, and a macroscopic carbon material is obtained at temperatures as high as 900 °C. Higher temperatures also purify and reorganize the carbon at the molecular scale. It is well known, however, that vitreous carbon is not graphitizable and remains in its glasslike state, even if it is heated at much higher temperatures.

Interestingly, the shrinkage induced by the pyrolysis is exactly compensated by the weight loss, as demonstrated previously [13]. In other words, the bulk density of the foams always remains the same, regardless of the HTT. The material shrinks, but the cell structure is strictly retained, as confirmed by a number of SEM images reported recently [13–18]. The contribution of the present work is measuring, over a wide range of temperature, the mechanical properties of the materials that have different initial bulk densities.

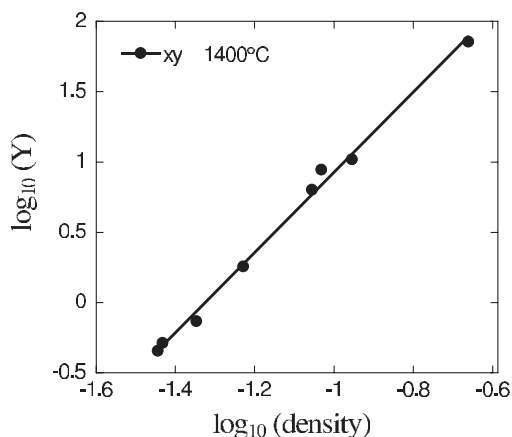


FIG. 3. Weight loss of tannin-based rigid foam, submitted to a thermal treatment in inert gas at 2 °C/min. At 1400 °C, the carbon yield is around 40%.

C. Measurement of the mechanical properties

Between 10 and 20 samples with various initial bulk densities were prepared for each HTT. Altogether, about 200 samples were prepared and characterized, of which 120 were analyzed. Half of the samples were investigated by compression along the z axis, while the other half were tested in the xy plane. The samples were compressed at a rate of 2 mm/min using an Instron 5944 universal testing machine equipped with a 2 kN head, and the strain-stress curves were recorded continuously.

The measured compression curves always exhibited the typical shape for cellular materials, whereas those measured for organic and carbon foams were characteristic of elastoplastic and elastic-brittle foams, respectively, according to the classification proposed by Gibson and Ashby [19]. A typical example is given in Fig. 4 for the organic and carbon foams for HTT = 900 °C, having similar densities close to 0.1 g/cm³

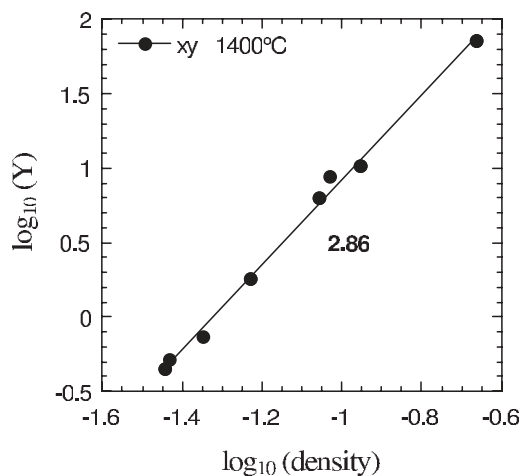


FIG. 4. Stress-strain characteristics of organic (nonheated) and carbon (HTT = 900 °C) foams, having a density close to 0.1 g/cm³ and tested along the xy direction. The elastic modulus is determined from the slope of the linear part (the inset for the organic foam), whereas the compressive strength is defined as the highest point of the plateau (the horizontal black arrows).

and compressed in the xy plane. As expected, both experiments and the results exhibit three regimes, namely, linear elasticity, collapse, and densification. The results for carbon foam are, however, clearly serrated in the plateau region, due to the fracture of successive layers of the brittle cells. Based on such data, the Young's modulus Y was estimated as the slope of the linear, initial part of the curves that represent the steepest slope (see the magnification of the first zone of the stress-strain curve in the inset of Fig. 4). The very beginning of the curve does correspond to parallelization of the opposite surfaces, submitted to the compressive stress, and thus, presents some irregularities. The compressive strength—also called yield strength or fracture stress [4]—was assumed to be the highest point of the long serrated plateau (see Fig. 4).

III. RESULTS AND DISCUSSION

We first present and discuss the results, and then analyze them based on percolation theory.

A. Mechanical properties of heat-treated foams

To our knowledge, up to now only the mechanical properties of organic and carbon foams, measured at 900°C , have been reported [17,18] that indicate clearly that the carbonization leads to tougher materials with both higher compressive strength σ and Young modulus Y , as indicated by Fig. 4. Intermediate and higher HTT lead to the strain-stress curves that are presented in Fig. 5 for a few samples that had bulk densities close to 0.05 g/cm^3 , and measured along the z direction. It can be seen that, on average, both the Young's modulus and the compressive strength increase with the HTT. Some exceptions may appear to exist to this general trend, but we consider them as either due to the scattering of the data, or because of the impossibility of preparing samples with exactly the same density that has strong influence on the mechanical properties, given that the percolation power laws with exponents that vary roughly from 2 to 4 are expected (see below).

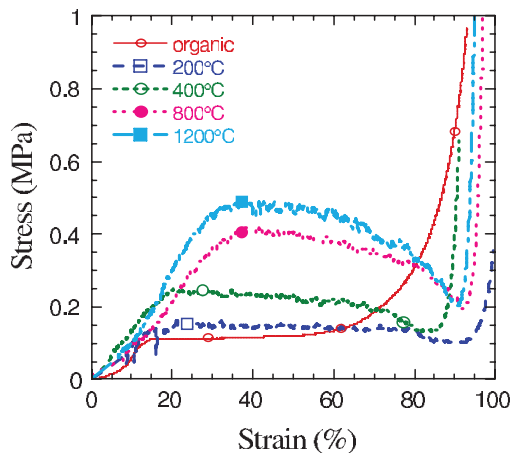


FIG. 5. (Color online) Stress-strain curves of the foams, submitted to various heat-treatment temperatures in a compression test. The samples have a bulk density of $0.050 \pm 0.005\text{ g/cm}^3$ and were tested along the z direction. “Organic” refers to the nontreated foam.

Close to 120 sets of results and curves similar to those presented in Fig. 5 were obtained for various densities, the HTT, and the two directions of the measurement. For all the cases the Young's modulus Y and the compressive strength σ were methodically estimated, as explained before. As discussed below, both properties always followed power laws as a function of the materials' bulk density.

B. The power laws and the exponents

Strictly speaking, the power laws (1) and (2) are supposed to be valid in the critical region very close to the percolation threshold. Thus, unlike computer simulations that, together with finite-size scaling, yield very precise estimates of the exponent τ and ζ , obtaining estimates of the two exponents through measurements is difficult, and therefore, one must be cautious about interpreting the physical implications of the estimated exponents.

The percolation threshold of the materials is zero. That is, regardless of how small ϕ was, the materials never lost their rigidity. Thus, for each HTT and each measurement direction (the xy planes or vertical direction z), the data for the Young's modulus Y and the compressive strength σ were plotted as $\log(Y)$ and $\log(\sigma)$ versus $\log(\phi)$, where ϕ is the density. In almost all cases, the range of $\log(\phi)$ was between -1.4 and -0.9 , corresponding to a typical range of density between 0.04 and 0.13 g/cm^3 . In a few cases, however, the density range was as broad as $0.035\text{--}0.22\text{ g/cm}^3$. The data were then fitted to a straight line. Figure 6 presents one example for the data at HHT = 1400°C , indicating that the linear correlation between $\log(Y)$ and $\log(\phi)$ is excellent. The same type of accurate linear regression was obtained for all the data that were analyzed, with no exception whatsoever. The errors due to the regression were all very small. For example, if we write the equation for the straight line in Fig. 6 as

$$\log(Y) = a + b \log(\phi), \quad (3)$$

we obtain $a \simeq 3.783 \pm 0.096$ and $b = \tau \simeq 2.856 \pm 0.082$. All the fits were obtained using the software KALEIDAGRAPH version 4.1.1. The correlation factor R^2 for all the fits was

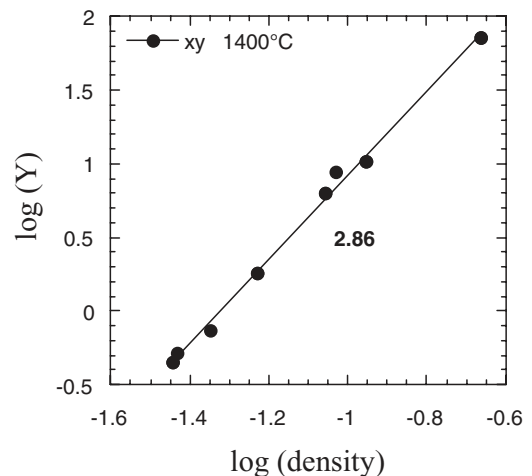


FIG. 6. An example of the log-log plot of the Young's modulus Y as a function of the density in the vicinity of the percolation threshold at the indicated heat-treatment temperature.

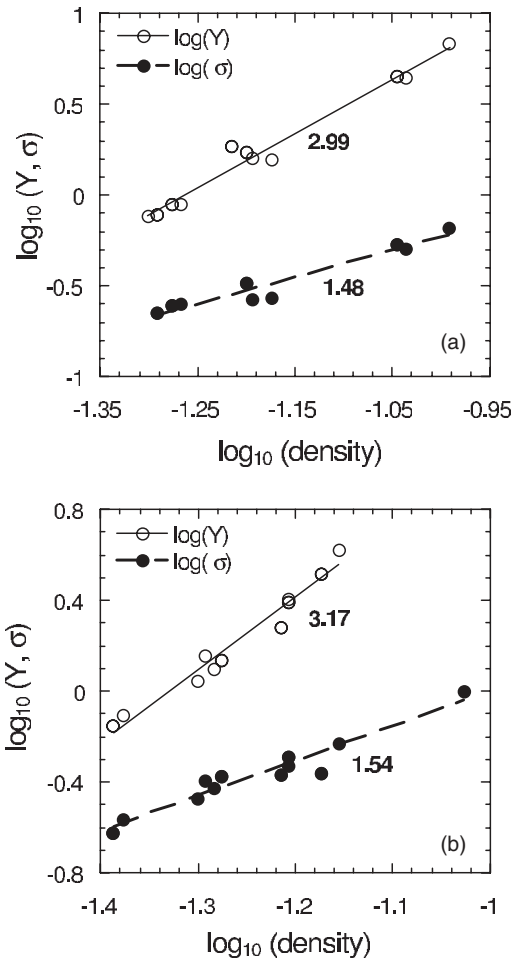


FIG. 7. Examples of the log-log plots of the Young's modulus Y and compressive strength σ as functions of the density. (a) Samples that were heat-treated at 200°C and measured in the xy plane. (b) Samples that were heat-treated at 800°C and measured along the z direction. The straight lines represent linear fits of the data with their slopes.

larger than 0.99, regardless of the HTT, the range of the density, and the measurement's direction, implying power laws for both Y and σ . Figure 7 presents two other examples of how the Young's modulus Y and the compressive strength σ vary as functions of the density at $\text{HTT} = 200$ and 800°C , exhibiting the same quality of goodness of the fit.

The resulting exponents of the corresponding power laws are gathered in Fig. 8 for all the HTTs, and include the non-heat-treated materials at 20°C . As pointed out earlier, given the scattering of the data, the related estimated error for each value of the exponent, and the narrow range over which power laws (1) and (2) are theoretically valid and the exponent can be measured reliably, interpretation of the implications of results in Fig. 8 must be done with caution. Despite this, some concrete observations may be made.

Figure 8(a) indicates that, in the case of the compressive strengths measured in the xy planes, the lowest value of the exponent ζ_{xy} that is for the material at $\text{HHT} = 400^\circ\text{C}$ is 1.3, while its highest value, at $\text{HHT} = 1200^\circ\text{C}$, is 1.7, both deviating from the theoretical value of 1.5 by about 13%. The average of all the values of ζ_{xy} is $\langle \zeta_{xy} \rangle \simeq 1.54$. With

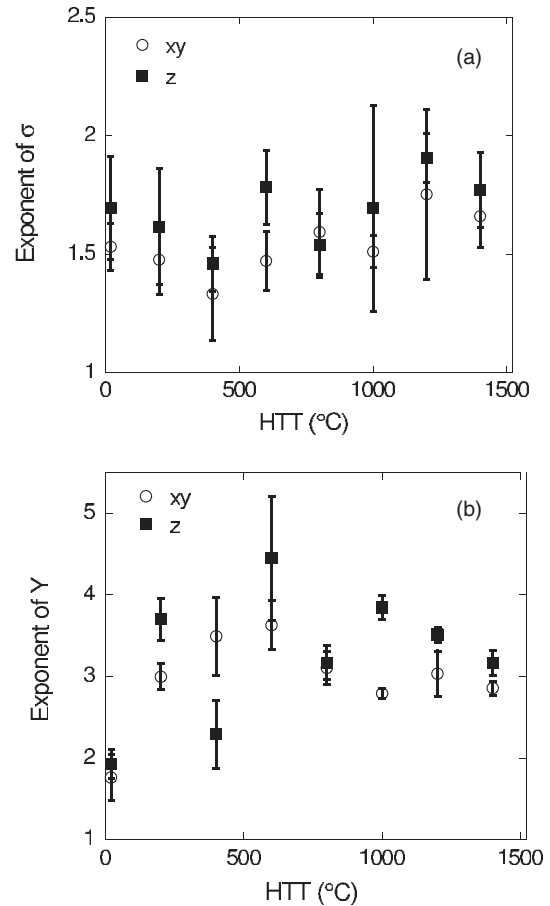


FIG. 8. The exponents of (a) the compressive strength σ and (b) the Young's modulus Y as functions of the HTT, the heat-treatment temperature.

only one exception, which occurs at $\text{HHT} = 800^\circ\text{C}$ where $\zeta_z \simeq \zeta_{xy}$, one has $\zeta_z > \zeta_{xy}$ for all the cases, although the trends of the variations of ζ_{xy} and ζ_z with the HHT are exactly the same, and the data are not precise enough to ascertain whether the difference is theoretically significant. The lowest and highest values of ζ_z are about 1.45 and 1.9, respectively. The average of all values of ζ_z is $\langle \zeta_z \rangle \simeq 1.68$. Thus, if we consider $\langle \zeta_z \rangle - \langle \zeta_{xy} \rangle \simeq 0.14$ as a measure of the material's anisotropy, it is, at least so far as σ is concerned, not strong.

Note that it has been conjectured [19] that ζ depends only on the structure of the material's pore space. The fact that the experiments yield an exponent between 1.5 and 2 seems to indicate that the foams' cells are intermediate between closed and open, as supported by the SEM images that indicate that the pores are connected by very narrow circular windows. This finding also supports the experimental observation that the structure remains unchanged during the entire pyrolysis process.

Essentially the same trends govern the dependence of the exponent τ of the Young's modulus Y in the xy planes and the vertical z direction, except that its direction dependence is a bit stronger than that of ζ , which also makes the interpretation of the results for τ more complex. First, we note that similar to ζ , except in one case at $\text{HHT} = 400^\circ\text{C}$, one always has $\tau_z > \tau_{xy}$. Moreover, just as $\zeta_z \simeq \zeta_{xy}$ at $\text{HHT} = 800^\circ\text{C}$, we

also have $\tau_z \simeq \tau_{xy}$ at the same HHT, hence indicating the internal consistency of the measurements and the data.

Consider estimates of τ_{xy} . The data indicate that τ_{xy} begins to increase from about 1.9 for the nonheated foams (at 20 °C), attains its maximum value at HHT = 600 °C, and then decreases to about 2.9 at 1000 °C, beyond which it remains more or less constant. As for ζ_z , the trends are more or less similar to those of τ_{xy} , except that in this case the maximum value of τ_z that is also attained at 700 °C is about 4.5 for which the estimated error is, however, large enough that τ_z and τ_{xy} overlap at 700 °C. The average of all the estimates of τ_{xy} at all the HHTs is $\langle \tau_{xy} \rangle \simeq 2.96$, whereas $\langle \tau_z \rangle \simeq 3.26$. Once again, the difference $\langle \tau_z \rangle - \langle \tau_{xy} \rangle$ indicates a small anisotropy.

The low-temperature value of τ corresponds to that of the 3D central-force (CF) model [6], which is also close to the critical exponent $t \simeq 2.0$ for the electrical conductivity of 3D systems. Within its estimated error, the maximum value of τ is close to 3.8, the exponent for the elastic moduli of 3D percolation models with CF and BB forces [8]. The estimated τ at the highest HHT and the averages τ_{xy} and τ_z are all close to 3, the mean-field value of the critical exponent for the electrical conductivity of percolation composites, which has also been suggested to be the mean-field value of τ for the elastic moduli of some gels [20].

Note that for some of the modified foam samples the estimate of τ is close to twice the corresponding τ for their organic precursors. As mentioned in the Introduction, according to the current understanding of the elastic properties of 3D solids near the percolation threshold, a change of τ may be expected if the nature of the elastic forces acting on the cellular solids also changes, or if the heat treatment changes the morphology of the material in a way that can give rise to nonuniversal value of the exponent τ of the elastic moduli [21].

Scaling analysis together with percolation theory predicts that the modulus exponent τ for highly porous materials, whose volume fraction of solid is close to the mechanical percolation threshold, is given by [22,23]

$$\tau = t + 2\nu, \quad (4)$$

where t is the critical exponent of the electrical conductivity of the material near the percolation threshold, and ν is the exponent of the percolation correlation length, $\xi_p \sim (p - p_c)^{-\nu}$. Equation (4) was proposed for the BB model, as well as the so-called beam model in which, in addition to the central and angle-changing forces, the torsional forces are also significant. Computer simulations indicate that for random 3D percolation, $\nu \simeq 0.89$ and $t \simeq 2.0$ [1,2]. Experiments with carbon foams [18] at HHT = 900 °C yielded $t \simeq 1.83$ and 1.64 for measurements along the z axis and in the xy planes, respectively, roughly consistent with Eq. (4).

Notwithstanding the relatively large error bars for some of the exponents, the possible nonuniversality of τ is surprising because, given that the experiments indicate that the pore structure of the materials does not change as they are heated up, the variations of τ cannot be attributed to the nonuniversality caused by a change in the pore structure [21]. Thus, the relatively significant dependence of the modulus exponent τ on the HHT is puzzling.

In an attempt to understand the variations of τ , several possibilities were considered. One way of interpreting the

changes in the modulus exponent τ might be based on the possible changes in the predominance of central forces over beamlike or angle-changing forces. However, if this were true, the changes should have been more gradual and smaller at lower temperatures, and not being already visible at HHTs as low as 200 °C, for which the transformation of the resin is also very slow.

Another possibility considered was the finite-size effects that can significantly affect the estimates of τ . Hence, we fitted the data for Y to the equation [24]

$$Y \sim (\phi - \phi_c)^\tau [a_1 + a_2(\phi - \phi_c)^{-\chi}], \quad (5)$$

where χ is a correction-to-scaling exponent, and a_1 and a_2 are two constants. Theoretically [24], one has $\chi \simeq 1.0$. The resulting estimates of τ were, however, similar to those presented in Fig. 8(b), except that the estimated errors were larger.

A third possibility is that the standard percolation exponents may correspond to a system at temperature $T = 0$, and thus at nonzero T , and in particular at high T in which the experiments were carried out, their numerical values may be different from the standard ones. Molecular dynamics (MD) simulation of randomly cross-linked monomers near the percolation threshold lends some support to this idea. It indicated [25] that the shear modulus of the material vanishes at the percolation threshold with an exponent that is close to that of the electrical conductivity, rather than the elastic moduli of percolation systems. Whether this can explain our data remains to be seen.

Yet, a fourth possibility is that, although the pore structure of the foam does not change significantly as the temperature rises, the internal structure of the solid matrix may change, as a result of which the values of the elastic moduli may change. But, to test this hypothesis one must carefully study the structure of the matrix as a function of the temperature, either during laborious experiments, or by careful MD simulations of the type that were recently used to study the pyrolysis of polymers [26].

IV. SUMMARY

Extensive data were reported for the elastic moduli of a cellular material whose composition was progressively varied while holding its pore structure unchanged. Rigid foam, prepared from a thermoset resin, was gradually converted into reticulated vitreous carbon foam by pyrolysis at increasingly higher heat-treatment temperatures. The Young's modulus Y and compressive strength σ of the material were measured as the temperature was raised. Near the rigidity or percolation threshold the data follow power laws as predicted by percolation theory, and the corresponding exponents were estimated. Whereas the exponent associated with the Young's modulus varies significantly with the heat-treatment temperature, the exponent associated with the compressive strength does not vary strongly with the HHT. Although the exponent τ associated with Y is within the range of the various estimates obtained by the scaling arguments and computer simulations, its apparent nonuniversality and dependence on the HHT remain unexplained.

ACKNOWLEDGMENTS

The authors gratefully acknowledge the financial support of the CPER 2007-2013 “Structuration du Pôle de Compétitivité

Fibres Grand” (Competitiveness Fibre Cluster), through local (Conseil Général des Vosges), regional (Région Lorraine), national (DRRT and FNADT), and European (FEDER) funds.

-
- [1] D. Stauffer and A. Aharony, *Introduction to Percolation Theory*, 2nd ed. (Taylor & Francis, London, 1994).
- [2] M. Sahimi, *Applications of Percolation Theory* (Taylor & Francis, London, 1994).
- [3] S. Torquato, *Random Heterogeneous Materials* (Springer, New York, 2002).
- [4] M. Sahimi, *Heterogeneous Materials I* (Springer, New York, 2003), Chap. 8.
- [5] S. Feng and P. N. Sen, *Phys. Rev. Lett.* **52**, 216 (1984); C. Moukarzel and P. M. Duxbury, *ibid.* **75**, 4055 (1995); D. J. Jacobs and M. F. Thorpe, *ibid.* **75**, 4051 (1995).
- [6] S. Arbabi and M. Sahimi, *Phys. Rev. B* **47**, 695 (1993).
- [7] Y. Kantor and I. Webman, *Phys. Rev. Lett.* **52**, 1891 (1984); S. Feng, P. N. Sen, B. I. Halperin, and C. J. Lobb, *Phys. Rev. B* **30**, 5386 (1984); S. Feng and M. Sahimi, *ibid.* **31**, 1671 (1985).
- [8] S. Arbabi and M. Sahimi, *Phys. Rev. B* **38**, 7173 (1988).
- [9] D. Deptuck, J. P. Harrison, and P. Zawadzki, *Phys. Rev. Lett.* **54**, 913 (1985); B. Gauthier-Manuel, E. Guyon, S. Roux, S. Gits, and F. Lefauchaux, *J. Phys. (Paris)* **48**, 869 (1987); T. Woignier, J. Phalippou, R. Sempere, and J. Pelons, *J. Phys. (France)* **49**, 289 (1988); F. Devreux, J. P. Boilot, F. Chaput, L. Malier, and M. A. V. Axelos, *Phys. Rev. E* **47**, 2689 (1993).
- [10] M. Adam, M. Delsanti, and D. Durand, *Macromolecules* **18**, 2285 (1985); S. Arbabi and M. Sahimi, *Phys. Rev. Lett.* **65**, 725 (1990).
- [11] J. Gross and J. Fricke, *Nanostruct. Mater.* **6**, 905 (1995).
- [12] W. S. Sanders and L. J. Gibson, *Mater. Sci. Eng., A* **347**, 70 (2003).
- [13] W. Zhao, A. Pizzi, V. Fierro, G. Du, and A. Celzard, *Mater. Chem. Phys.* **122**, 175 (2010).
- [14] G. Tondi, W. Zhao, A. Pizzi, G. Du, W. Fierro, and A. Celzard, *Bioresour. Technol.* **100**, 5162 (2009).
- [15] A. Celzard, V. Fierro, G. Amaral-Laba, A. Pizzi, and J. Torero, *Polym. Degrad. Stab.* **96**, 477 (2011).
- [16] G. Tondi, S. Blacher, A. Léonard, A. Pizzia, V. Fierro, J. M. Lebana, and A. Celzard, *Microsc. Microanal.* **15**, 384 (2009).
- [17] A. Celzard, W. Zhao, A. Pizzi, and V. Fierro, *Mater. Sci. Eng., A* **527**, 4438 (2010).
- [18] W. Zhao, V. Fierro, A. Pizzi, G. Du, and A. Celzard, *Mater. Chem. Phys.* **123**, 210 (2010).
- [19] L. J. Gibson and M. F. Ashby, *Cellular Solids: Structure and Properties*, 2nd ed. (Cambridge University Press, London, 1997), p. 177.
- [20] M. Daoud and A. Coniglio, *J. Phys. A* **14**, L301 (1981); E. Del Gado, L. de Arcangelis, and A. Coniglio, *Europhys. Lett.* **46**, 288 (1999).
- [21] B. I. Halperin, S. Feng, and P. N. Sen, *Phys. Rev. Lett.* **54**, 2391 (1985); S. Feng, B. I. Halperin, and P. N. Sen, *Phys. Rev. B* **35**, 197 (1987).
- [22] M. Sahimi, *J. Phys. C* **19**, L79 (1986).
- [23] S. Roux, *J. Phys. A* **19**, L351 (1986).
- [24] M. Sahimi and S. Arbabi, *J. Stat. Phys.* **62**, 453 (1991).
- [25] M. Plischke, *Phys. Rev. E* **73**, 061406 (2006).
- [26] S. Naserifar, L. Liu, W. A. Goddard, T. T. Tsotsis, and M. Sahimi, *J. Phys. Chem. C* **117**, 3308 (2013); S. Naserifar, W. A. Goddard, L. Liu, T. T. Tsotsis, and M. Sahimi, *ibid.* **117**, 3320 (2013).